THE JOURNAL OF BIOLOGICAL CHEMISTRY
Vol. 278, No. 1, Issue of January 3, pp. 444–453, 2003
Printed in U.S.A.

Protein Kinase A Phosphorylation of the Cardiac Calcium Release Channel (Ryanodine Receptor) in Normal and Failing Hearts

ROLE OF PHOSPHATASES AND RESPONSE TO ISOPROTERENOL*

Received for publication, July 13, 2002
Published, JBC Papers in Press, October 24, 2002, DOI 10.1074/jbc.M207028200

Steven Reiken‡, Marta Gaburjakova‡§, Silvia Guatimosim¶, Ana M. Gomez‖, Jeanine D'Armiento‡, Daniel Burkhoff, Jie Wang**, Guy Vassort‖, W. Jonathan Lederer¶, and Andrew R. Marks‡ ‡‡§§**

*From the ‡Center for Molecular Cardiology, the ‡‡Department of Pharmacology, the **Circulatory Physiology Division, Department of Medicine, Columbia University College of Physicians and Surgeons, New York, New York 10032, the ¶Medical Biotechnology Center, University of Maryland Biotechnology Institute, Department of Physiology, School of Medicine, University of Maryland, Baltimore, Maryland 21201, ‖Physiopathologie Cardiovasculaire, INSERM, Montpellier 34295, France, and the §Institute of Molecular Physiology and Genetics, Slovak Academy of Science, Bratislava 83334, Slovak Republic*

The cardiac ryanodine receptor/calcium release channel (RyR2) on the sarcoplasmic reticulum (SR) comprises a macromolecular complex that includes a kinase and two phosphatases that are bound to the channel via targeting proteins. We previously found that the RyR2 is protein kinase A (PKA)-hyperphosphorylated in end-stage human heart failure. Because heart failure is a progressive disease that often evolves from hypertrophy, we analyzed the RyR2 macromolecular complex in several animal models of cardiomyopathy that lead to heart failure, including hypertrophy, and at different stages of disease progression. We now show that RyR2 is PKA-hyperphosphorylated in diverse models of heart failure and that the degree of RyR2 PKA phosphorylation correlates with the degree of cardiac dysfunction. Interestingly, we show that RyR2 PKA hyperphosphorylation can be lost during perfusion of isolated hearts due to the activity of the endogenous phosphatases in the RyR2 macromolecular complex. Moreover, infusion of isoproterenol resulted in PKA phosphorylation of RyR2 in rat, indicating that systemic catecholamines can activate phosphorylation of RyR2 *in vivo*. These studies extend our previous analyses of the RyR2 macromolecular complex, show that both the kinase and phosphatase activities in the macromolecular complex are regulated physiologically *in vivo*, and suggest that RyR2 PKA hyperphosphorylation is likely a general feature of heart failure.

During the "fight or flight" response, sympathetic nervous system activation modulates the signaling pathway that controls excitation-contraction (EC)[1] coupling in the heart resulting in increased cardiac output required to meet stress-induced increases in metabolic demands. EC coupling in heart muscle converts electrical signals to mechanical ones via elevation of cytosolic calcium (Ca^{2+}), which triggers contraction. The major components that regulate cardiac EC coupling are all modulated by activation of the sympathetic nervous system via phosphorylation by adenosine 3′,5′-monophosphate (cAMP)-dependent protein kinase (PKA). These include: 1) the triggers for EC coupling, predominantly Ca^{2+} influx through the voltage-gated Ca^{2+} channel (dihydropyridine receptor) on the plasma membrane and possibly Ca^{2+} influx via the Na^{+}-Ca^{2+} exchanger; 2) the SR Ca^{2+} release channel or type 2 ryanodine receptor (RyR2); and 3) the SR Ca^{2+} reuptake pump (SERCA2a) and its regulatory protein phospholamban (PLB). Although the roles of the sarcolemmal Ca^{2+} channel and PLB phosphorylation are well established, the physiological significance of RyR2 PKA phosphorylation is not yet fully understood.

RyR2 is one of the largest known ion channels. Each RyR2 has an enormous cytoplasmic domain that serves as a scaffold for regulator proteins that modulate the channel's activity (1). The RyR2 cytoplasmic scaffold domain contains highly conserved leucine/isoleucine zippers that bind to leucine/isoleucine zippers present in the adaptor/targeting proteins for kinases (PKA) and phosphatases (PP1 and PP2A) that regulate RyR channel function (1). In 1989 Marks *et al.* (2) discovered a 12-kDa protein that co-purifies with RyR1 and was later shown to be FKBP12, the cytosolic binding protein for the immunosuppressant drugs FK506 and rapamycin (3–5). A 12.6-kDa isoform of FKBP12 (FKBP12.6) is tightly associated with RyR2 and modulates its function, possibly by enhancing cooperativity among its four subunits (4, 6–8). Four FKBP molecules are part of each RyR channel (9). So, in fact, RyR2 is a macromolecular complex containing kinases, phosphatases, and FKBP.

The sympathetic nervous system is activated in response to stress, resulting in increased levels of local and circulating catecholamines that activate β-adrenergic receptors (β-AR),

* This work was supported in part by grants (to A. R. M., W. J. L., and J. D.) from the National Institutes of Health and the Whitaker Foundation (to S. R.). The costs of publication of this article were defrayed in part by the payment of page charges. This article must therefore be hereby marked "*advertisement*" in accordance with 18 U.S.C. Section 1734 solely to indicate this fact.

§§ The Doris Duke Charitable Foundation Distinguished Clinical Scientist. To whom correspondence should be addressed: Center for Molecular Cardiology, Box 65, Columbia University College of Physicians & Surgeons, Rm. 9-401, 630 W. 168th St., New York, NY 10032. Tel.: 212-305-0270; Fax: 212-305-3690; E-mail: arm42@columbia.edu.

[1] The abbreviations used are: EC, excitation-contraction; PKA, protein kinase A; RyR2, ryanodine receptor/calcium release channel; PLB, phospholamban; PP1 and PP2A, phosphatase 1 and 2A; FKBP, cytosolic binding protein for the immunosuppressant drugs FK506 and rapamycin; AR, adrenergic receptor; SR, sarcoplasmic reticulum; SERCA2a, SR Ca^{2+} reuptake pump; EAD, early after depolarization; DAD, delayed after depolarization; PKI, PKA inhibitor; PMI, post-myocardial infarction; ANOVA, analysis of variance; MMP-1, matrix metalloproteinase type 1; WT, wild type; TG, transgenic; CRU, Ca^{2+} release unit; HF, heart failure; Iso, isoproterenol; PIPES, piperazine-*N*,*N*′-bis(2-ethanesulfonic acid).

elevate intracellular cAMP, and activate PKA. PKA phosphorylation modulates RyR2 function both *in vitro* and *in vivo* (1, 10–20). Channels from failing hearts have been shown to be PKA-hyperphosphorylated leading to dissociation of the FKBP12.6 and altered RyR2 channel function (14–16, 21). Thus, maladaptation of a classic physiological pathway ("fight or flight" that has never been subjected to evolutionary pressure, because heart failure is a new disease of the last century or two) plays an important role in the pathophysiology of heart failure, which is a chronic hyperadrenergic state (15, 21). PKA hyperphosphorylation of RyR2 in failing hearts shifts the sensitivity of RyR2 to Ca^{2+} to the left (16) resulting in "leaky" channels that can deplete SR Ca^{2+} stores and contribute to reduced Ca^{2+} transients that may impair contractility. If conditions lead to transient SR Ca^{2+} overload, then the SR Ca^{2+} leak during repolarization may contribute to "early after depolarizations" (EADs) and during diastole initiate "delayed after depolarizations" (DADs) by activating "transient inward currents" (22). EADs and DADs can trigger fatal cardiac arrhythmias (*e.g.* ventricular tachycardia) (23–25). How Ca^{2+} signaling pathways interact to produce alterations in the $[Ca^{2+}]_i$ transient observed in heart failure is not well understood. Here we examine how RyR2 PKA phosphorylation is regulated and how this form of regulation may be linked to changes in RyR2 function.

PKA hyperphosphorylation of RyR2 also decreases coupled gating between RyR2 (26, 27) due to dissociation of FKBP12.6 from the channel. Reduced coupled gating may lead to incomplete closure of RyR2 following activation (14, 15) that would tend to decrease SR Ca^{2+} content. Administration of oral β-AR blockers reverses the PKA hyperphosphorylation of RyR2, restores normal stoichiometry of the RyR2 macromolecular complex, and restores normal single channel function in a canine model of heart failure (28).

Here we analyze the RyR2 PKA phosphorylation and the RyR2 macromolecular complex in several models of heart failure, including hypertrophy that leads to heart failure, and at different stages of the disease. We now show that, in isolated perfused rodent hearts, inhibition of endogenous phosphatase activity results in a significant increase in PKA phosphorylation of RyR2 in response to isoproterenol, indicating that phosphatases are indeed active in the RyR2 macromolecular complex in intact heart. Moreover, infusion of isoproterenol resulted in PKA phosphorylation of RyR2 in rat, indicating that systemic catecholamines can activate phosphorylation of RyR2 *in vivo*. Using a rat model of myocardial infarction-induced heart failure, we demonstrate that RyR2 is PKA-hyperphosphorylated while in the same hearts phospholamban is PKA-hypophosphorylated. Using this model we further show that the RyR2 macromolecular complex is depleted of FKBP12.6 and PP1 and PP2A. RyR2 PKA hyperphosphorylation was also demonstrated in a murine model of cardiac-specific β2-AR overexpression confirming that the hyperphosphorylation of RyR2 is due to activated PKA. Moreover, a murine cardiomyopathy model in which cardiac dysfunction is associated with expression of collagenase in the heart also results in PKA hyperphosphorylation of RyR2 that is progressive over time and correlates with the degree of cardiac dysfunction. These studies extend our previous studies on the RyR2 macromolecular complex and show that the both the kinase and phosphatase activities in the macromolecular complex can be regulated physiologically *in vivo*.

MATERIALS AND METHODS

Immunoprecipitation and Back-phosphorylation of Ryanodine Receptor—Heart homogenates were prepared by homogenizing ~1.0 g of cardiac tissue in 1.0 ml of a buffer containing 50 mM Tris-HCl (pH 7.4), 200 mM NaCl, 20 mM NaF, 1.0 mM Na_3VO_4, 1.0 mM dithiothreitol, and protease inhibitors. Samples were centrifuged at 3000 × *g* for 10 min. After determining the protein concentration, the supernatants were aliquoted and stored at −80 °C until use. RyR2 was immunoprecipitated from heart samples by incubating 500 μg of homogenate with anti-RyR antibody in 0.5 ml of a modified radioimmunoprecipitation assay buffer (50 mM Tris-HCl (pH 7.4), 0.9% NaCl, 5.0 mM NaF, 1.0 mM Na_3VO_4, 0.25% Triton X-100, and protease inhibitors) overnight at 4 °C. Protein A-Sepharose beads were added, incubated at 4 °C for 1 h, washed with 1× phosphorylation buffer (8 mM $MgCl_2$, 10 mM EGTA, and 50 mM Tris/PIPES, pH 6.8), and resuspended in 10 μl of a 1.5× phosphorylation buffer containing either PKA catalytic subunit (Sigma Chemical Co., St. Louis, MO) or PKA plus a PKA inhibitor (PKI_{5-24}, 500 nM, Calbiochem, San Diego, CA). Back-phosphorylation of immunoprecipitated RyR2 was initiated with 33 μM Mg-ATP containing 10% [γ-^{32}P]ATP (PerkinElmer Life Sciences, Boston, MA) and terminated after 8 min at room temperature with 5 μl of stop solution (4% SDS and 0.25 M dithiothreitol). Samples were heated to 95 °C, size-fractionated on 6% SDS-PAGE, and RyR2 radioactivity was quantified using a PhosphorImager and ImageQuaNT software (Amersham Biosciences, Piscataway, NJ). Nonspecific phosphorylation (not inhibited by PKA inhibitor) was subtracted, and the resulting value was divided by the amount of RyR2 protein and expressed as the inverse of the PKA-dependent [γ-^{32}P]ATP signal.

Immunoblot—Proteins were size-fractionated on 6% SDS-PAGE for RyR, 12% SDS-PAGE for RII, PKA, PP1, and PP2A, and 15% SDS-PAGE for phospholamban and FKBP12.6. Immunoblots were developed using Anti-RyR (Affinity Bioreagents, Golden, CO, 1:3000 dilution in 5% milk-TBS-Tween), a phosphospecific phospholamban antibody (Cyclacel Limited, Dundee, Scotland, 1:5000 dilution in 5% milk-TBS-Tween), anti-RII (1:1000), anti-PKA catalytic subunit (1:1000), anti-PP1 (1:1000), anti-PP2A (Transduction Laboratories), and anti-FKBP (1:1000).

Isoproterenol Infusion of Rats—Rats were anesthetized with a mixture of intraperitoneal 100 mg/kg ketamine and 10 mg/kg xylazine. Vessel cannulation was performed using a 2-cm longitudinal incision made below the mandible to the thoracic inlet. The left internal jugular vein was isolated and cannulated with an Intramedic PE-10 polyethylene catheter. Isoproterenol hydrochloride (0.2 mg/ml) was infused through the venous catheter at a rate ranging from 0.1 to 1.0 ml/min until the mean arterial pressure decreased to 60% of baseline.

Rat Infarct Model—Male Wistar rats (180–200 g) were used to produce myocardial infarction as described previously (29). Briefly, rats were anesthetized with a mixture of 150 mg/kg intraperitoneal ketamine and 15 mg/kg chlorpromazine. Respiration was maintained with a ventilation assist device and an endotracheal tube (3 ml air/60 strokes per minute). After median-left thoracotomy and pericardium opening, the left main coronary artery was occluded with a 7-0 silk suture at the most proximal point below the left atria appendage. Sham-operated rats were treated the same way but without coronary artery ligation. Animals were euthanized for experiments at 6-month post-ligation. Before they were euthanized, animals underwent hemodynamic measurements or echocardiography.

Cardiomyocyte Isolation and Calcium Spark Measurements—Ventricular cardiac myocytes were isolated from control and PMI myocytes by standard enzymatic (collagenase Worthington type II, 1 mg/ml) methods. After isolation, cells from the left ventricular free wall (around the infarction) were stored in DEM media (1.8 mM $CaCl_2$). The cells were loaded with the fluorescence Ca^{2+} dye Fluo-3 through the patch-clamp pipette. Data are shown as the ratio of measured fluorescence (F) over fluorescence min (F_o). All images were acquired with a Bio-Rad MRC 600 confocal microscope fitted with an argon laser and processed with Bio-Rad SOM, COMOS, and IDL (Research Imaging Systems, Boulder, CO) software. Ca^{2+} sparks were evoked by depolarizations to voltages close to the activation threshold of I_{Ca} using an Axopatch 200A patch-clamp amplifier and recorded using pClamp 6.01 (Axon Instruments). Holding potential was −80 mV, then a ramp (500 ms) to −45 mV was applied to inactivate Na^+ channels, and 200-ms depolarizations were applied in 2-mV steps until no individual sparks but a global $[Ca^{2+}]_i$ transient was evoked. Series resistance was electronically compensated to 40–60%.

Cells were superfused with an external solution containing (in mM) NaCl 135; $MgCl_2$ 1; CsCl 20; glucose 10; HEPES 10; $CaCl_2$ 1.8 (pH 7.4). When isoproterenol was used, 10 μM tetrodotoxin was used to block Na^+ channels. Patch pipettes were filled with (in mM) CsCl 130; fluo-3 0.05; HEPES 10; $MgCl_2$ 0.33; triethanolamine-Cl 20; Mg-ATP 4 (pH 7.2). Temperature was maintained at 35–37 °C throughout each experiment.

Perfusion of Normal Rat Hearts—Briefly, male Sprague-Dawley rats

weighing between 250 and 300 g were euthanized by lethal injection of pentobarbital sodium (100 mg/kg). The hearts were rapidly removed and perfused via the Langendorff method with Ca^{2+}-free modified Tyrode's solution containing (mM) NaCl 137, KCl 5, HEPES 20, $MgCl_2$ 0.5, glucose 15, and NaH_2PO_4 1 with pH 7.4 at 37 °C for 5 min until the blood was washed out. Hearts were then perfused with 1 μM isoproterenol for 15 min or identical procedure in the complete absence of isoproterenol. The same procedure was repeated in the presence of 1 mM NaF during the whole perfusion (20 min) with or without isoproterenol (1 μM). Following perfusion, the heart ventricles were removed and quickly frozen (liquid nitrogen) until further use.

Perfusion of Hypertrophic Hearts—Dahl salt-sensitive (SS) and Dahl salt-resistant (control, Dahl SR/Jr) rats were fed an 8% high salt diet from 6 weeks of age as described previously (30). SS Dahl rats develop severe hypertension and concentric compensated hypertrophy over a period of weeks when fed a high salt diet, the SR/Jr strain do not develop hypertension or cardiac hypertrophy. After 8 weeks on diet the rats were sacrificed, and the hypertrophic hearts were perfused using the procedure described above with or without 1 mM NaF in the perfusate as indicated, except that no isoproterenol was added to the perfusion solution.

Single Channel Recordings—Single channel recordings of RyR2 were performed and analyzed under voltage-clamp conditions as described previously (16). We used planar lipid bilayers consisting of 3:1 phosphatidylethanolamine:phosphatidylserine (Avanti Polar Lipids, 20 mg/ml) formed across a 0.15-mm aperture in a polystyrene cup (Warner Instruments). SR membrane vesicles were added to the *cis* (cytoplasmic) side of the membrane and induced to fuse with the lipid bilayer by increasing KCl concentration to 800 mM. After incorporation of vesicles with channels to bilayer, the KCl gradient across the bilayer was eliminated by perfusion of the *cis* chamber with *cis* solution. Solutions used for channel analysis were: *trans* solution, 250 mM Hepes, 53 mM $Ca(OH)_2$, and 50 mM KCl (pH 7.4); *cis* solution, 250 mM HEPES, 125 mM Tris, 50 mM KCl, 1 mM EGTA, 0.5 mM $CaCl_2$ (pH 7.4). Free [Ca^{2+}] (*cis*) 150 nM was calculated using CHELATOR software (31). The *trans* chamber of the lipid bilayer was connected to the head-stage input of an Axopatch 200A amplifier (Axon Instruments) using an Ag/AgCl electrode and an agarose/KCl bridge. The *cis* side was held at ground with a similar electrode. The single-channel currents were filtered at 1 kHz with a four-pole Bessel filter (Warner Instruments) and digitized with a 4-kHz sampling frequency using a DigiData 1200 interface (Axon Instruments) with AxoScope1 software (Axon Instruments). At the conclusion of each experiment, ryanodine or ruthenium red were applied to confirm the identity of channels as RyR2. pClamp 6.0.3 software (Axon Instruments) was used for analyzing channel records. Open probability (P_o) and open and closed dwell times were identified using a 50% threshold analysis from at least 2 min of continual records. To find mean dwell times (τ_i) and their proportions (area under the curve for each exponential distribution), the dwell time distributions were fitted using the Levenberg-Marquardt least-squares method with SigmaPlot 4.00 software (Jandel Scientific). Distributions were generated by pooling data for individual channels ($n > 3$) to get precise fitted parameters. The *F* test was employed for statistical comparisons of different kinetics models. Events shorter than 500 μs were excluded from analyses. Results are presented as mean ± S.D.; Student's *t* test or ANOVA (where indicated) was used for statistical analyses. The unpaired *t* test or Welch *t* test were used for statistical analysis. Mean dwell times are presented as the value of the fitted coefficient ± S.E. (S.E. represents the uncertainty in the estimates of the fitted coefficient). A *p* value less than 0.05 was considered statistically significant.

RESULTS

Given the strong evidence showing PKA hyperphosphorylation of RyR2 in heart failure as noted above (16, 28), it was initially hard to reconcile the findings of Gomez *et al.* (30) who reported that RyR2 function was normal in preparations obtained from animals in heart failure. To resolve this paradox, we explored the hypothesis that it may be necessary to prevent dephosphorylation of RyR2 by phosphatases to observe the PKA phosphorylated state of RyR2 in isolated cardiomyocytes. Fig. 1*A* shows the result of an experiment that investigates this process. Phosphorylation of RyR2 and phospholamban (PLB) were examined. Langendorff perfusion of a control heart with isoproterenol (1 μM) only produced PKA phosphorylation of RyR2, if the weak phosphatase inhibitor NaF (1 mM) was

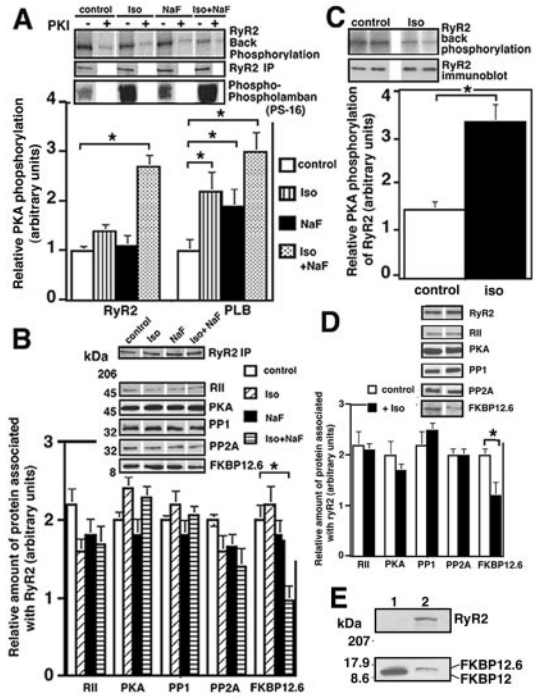

FIG. 1. **Isoproterenol induces PKA phosphorylation of RyR2 and phospholamban in intact hearts.** Rat hearts were perfused via the Langendorff method with Ca^{2+}-free modified Tyrode's solution containing isoproterenol 1 μM (*Iso*), the phosphatase inhibitor sodium fluoride 1 mM (*NaF*), NaF plus Iso, or buffer. In *A*: The *upper panel* shows an autoradiogram of back-phosphorylation of immunoprecipitated RyR2 with PKA and [γ-^{32}P]ATP with or without PKA inhibitor (*PKI*). The *middle panel* shows an immunoblot of immunoprecipitated RyR2 to confirm that equivalent amounts of RyR2 protein were present in each back-phosphorylation assay. The *lower panel* shows an immunoblot of heart lysate with anti-phospholamban antibody that detects the phosphorylation of serine 16 (*PS-16*). The *bar graph* shows the relative PKA phosphorylation of RyR2 and phospholamban in the various treatment groups. In *B*: The *upper panels* are immunoblots of immunoprecipitations using anti-RyR antibody (5029) showing levels of components of the RyR2 macromolecular complex including RyR2, the PKA regulatory subunit RII, PKA catalytic subunit, PP1, PP2A, and FKBP12.6. The accompanying *bar graph* shows the relative amounts of each of the components of the RyR2 macromolecular complex in response to control, Iso, NaF, and Iso plus NaF. *C*, RyR2 PKA phosphorylation was measured following infusion of isoproterenol via the jugular vein in rats ($n = 2$). *D*, *upper panels* are immunoblots of immunoprecipitations using anti-RyR antibody (5029) showing levels of components of the RyR2 macromolecular complex, including RyR2, the PKA regulatory subunit RII, PKA catalytic subunit, PP1, PP2A, and FKBP12.6. The accompanying *bar graph* shows the relative amounts of each of the components of the RyR2 macromolecular complex in response to isoproterenol infusion. *E*, immunoblot showing: *lane 1*, FKBP12.6 and FKBP12 both detected in human cardiac homogenate (50 μg) using an anti-FKBP antibody that recognizes both proteins; *lane 2*, an immunoprecipitation from the same cardiac homogenate (300 μg) using an anti-RyR-5029 antibody showing that only FKBP12.6 co-immunoprecipitates with RyR2 in heart. The *top half* of the gel was immunoblotted with anti-RyR antibody; the *bottom half* was immunoblotted with anti-FKBP12 antibody. RyR2 is not seen in *lane 1* because insufficient cardiac homogenate was added. *, $p < 0.01$ for the indicated comparison.

present. NaF perfusion alone did not produce RyR2 phosphorylation. In contrast, PLB was phosphorylated by isoproterenol in the presence or absence of NaF. This finding suggests that studies performed on isolated cardiomyocytes that are harvested following a similar Langendorff perfusion do not accurately represent the phosphorylation status of RyR2 in the intact heart due to continuing activity of the bound phosphatases during the perfusion. In contrast, phospholamban, a small protein that does not have phosphatases and kinases targeted directly to it, is regulated differently from RyR2 with respect to

phosphorylation and dephosphorylation in the isolated perfused heart.

PKA phosphorylation of RyR2 leads to dissociation of FKBP12.6 from the channel resulting in altered RyR2 function. Therefore, it is important to test what, if any, changes in the macromolecular complex take place following the treatment of Langendorff-perfused control hearts with isoproterenol as shown in Fig. 1*A*. To assess the effect of acute PKA phosphorylation of RyR2 in an intact heart on the RyR2 macromolecular complex we immunoprecipitated the complex from the perfused rat hearts with an anti-RyR2 antibody and immunoblotted for components of the RyR2 macromolecular complex (Fig. 1*B*). All of the components of the macromolecular complex are shown to remain at the same levels as in control (non-isoproterenol-treated) except FKBP12.6. FKBP12.6 was reduced by about 40% following perfusion with isoproterenol and NaF, but there was no significant reduction following perfusion by either isoproterenol or NaF alone. These findings are consistent with the depletion of FKBP12.6 from the RyR2 complex due to the PKA hyperphosphorylation of RyR2 in heart failure (16). The notable difference between the acute PKA phosphorylation of RyR2 shown here and the longer-term PKA phosphorylation of RyR2 in heart failure are the reductions of the phosphatases PP1 and PP2A in heart failure (16) that were not observed following acute PKA phosphorylation due to isoproterenol perfusion (Fig. 1*A*). This finding suggests that the acute effect of isoproterenol-induced PKA phosphorylation of RyR2 is to deplete the complex of FKBP12.6. The reduction in phosphatase levels in the RyR2 macromolecular complex that we have observed in channels from failing hearts (16) represents a distinct effect of the chronic hyperadrenergic state of heart failure that is not completely recapitulated with acute perfusion with isoproterenol.

An important question that needs to be addressed is whether or not RyR2s in the heart become PKA-phosphorylated following systemic infusion of isoproterenol in the intact animal? Infusion of isoproterenol hydrochloride (0.2 mg/ml) at a rate ranging from 0.1 to 1.0 ml/min was conducted until the mean arterial pressure decreased to 60% of baseline at which point the animals were sacrificed, and the hearts were excised and immediately flash-frozen so that there was no time for phosphatases bound to RyR2 to dephosphorylate the channel. Under these conditions isoproterenol infusion resulted in a significant increase in PKA phosphorylation of RyR2 (Fig. 1*C*). Isoproterenol infusion reduced the amount of FKBP12.6 bound to the RyR2 complex but did not alter levels of PKA, RII, PP1, or PP2A (Fig. 1*D*). Although both FKBP12 and FKBP12.6 are expressed in the heart, and FKBP12 is considerably more abundant than FKBP12.6, only FKBP12.6 co-immunoprecipitated with RyR2 (Fig. 1*E*). These data provide compelling evidence that β-AR activation leads to RyR2 PKA phosphorylation and the dissociation of FKPB12.6.

Investigation of the phosphorylation/dephosphorylation balance hypothesis to understand PKA hyperphosphorylation of RyR2 in cardiac hypertrophy and failure requires use of more than one model. To assess the PKA phosphorylation state of RyR2 and phospholamban in a hypertrophic cardiomyopathy model, the salt-sensitive (SS) Dahl rat was used. SS Dahl rats were maintained on a high salt diet for 8 weeks to produce hypertension and cardiac hypertrophy. Hearts from these animals were isolated and perfused using the Langendorff method and compared with hearts from control animals (age-matched strain that remains normotensive on the same high salt diet, Dahl SR/Jr). Following Langendorff perfusion, hyperphosphorylation of RyR2 was observed in Dahl rat hearts in the presence of NaF (1 mM) but not in its absence and not in control. In

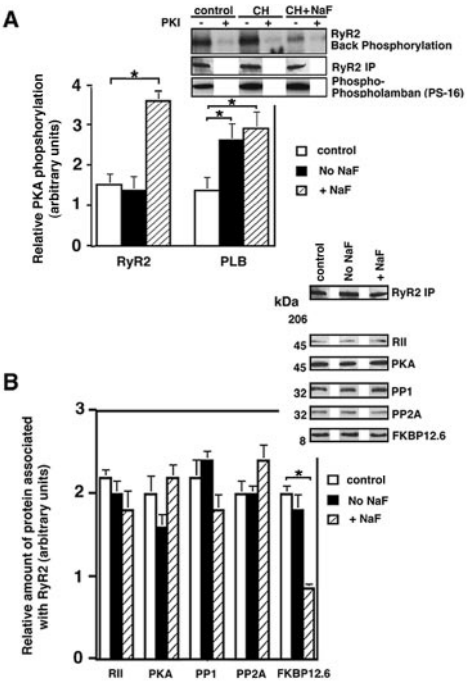

FIG. 2. **PKA hyperphosphorylation of RyR2 in cardiomyopathic hearts.** Cardiomyopathic hearts (*CH*) from salt-sensitive (*SS*) Dahl rats maintained on a high salt diet for 8 weeks were perfused via the Langendorff method with Ca^{2+}-free modified Tyrode's solution or Tyrode's solution containing 1 mM NaF (*CHF + NaF*). Controls were Dahl salt-resistant (*SR/Jr*) rats maintained on the same high salt diet. *A*, *upper panel* shows autoradiogram of back-phosphorylation of immunoprecipitated RyR2 with PKA and [γ-^{32}P]ATP with or without PKA inhibitor (*PKI*). The *middle panel* shows an immunoblot of immunoprecipitated RyR2 to confirm that equivalent amounts of RyR2 protein were present in each back-phosphorylation assay. The *lower panel* shows an immunoblot of heart lysate with anti-phospholamban antibody, which detects the phosphorylation of serine 16 (*PS-16*). The *bar graph* shows the relative PKA phosphorylation of RyR2 and phospholamban in the various treatment groups. *B*, *upper right panels* are immunoblots of immunoprecipitations using anti-RyR antibody (5029) showing levels of components of the RyR2 macromolecular complex, including RyR2, the PKA regulatory subunit RII, PKA catalytic subunit, PP1, PP2A, and FKBP12.6. The accompanying *bar graph* shows the relative amounts of each of the components of the RyR2 macromolecular complex in hearts perfused with or without NaF (1 mM). *, $p <$ 0.01 for the indicated comparison.

contrast, phospholamban was PKA-phosphorylated whether or not NaF was added to the perfusate (Fig. 2*A*). These data show that RyR2 and PLB are differentially regulated with respect to PKA phosphorylation in the severe hypertrophy of the Dahl-hypertensive rat. Importantly, these data are the first to show that RyR2 can be PKA-hyperphosphorylated in severe cardiac hypertrophy and that this is not just a feature found in end-stage heart failure. Moreover, this is the fist report of a condition in which both RyR2 and PLB are PKA-hyperphosphorylated in the same cardiomyopathy (in contrast to heart failure in which RyR2 is PKA-hyperphosphorylated but PLB is not).

The RyR2 macromolecular complex was examined using immunoprecipitation with an anti-RyR2 antibody followed by immunoblotting for components of the RyR2 macromolecular complex (Fig. 2*B*). We found a reduction of ~40% in the amount of FKBP12.6 ($p < 0.001$) in the RyR2 macromolecular complex that correlated with the increase in PKA phosphorylation of RyR2 (Fig. 2*A*). However, the levels of the phosphatases PP1 and PP2A were not significantly decreased (Fig. 2*B*) suggesting that hypertrophic cardiomyopathy-induced PKA phosphorylation of RyR2 differs from that seen in failing hearts in which we have previously documented a reduction in phosphatase levels in the RyR2 macromolecular complex (16). In this matter, the Dahl rat more

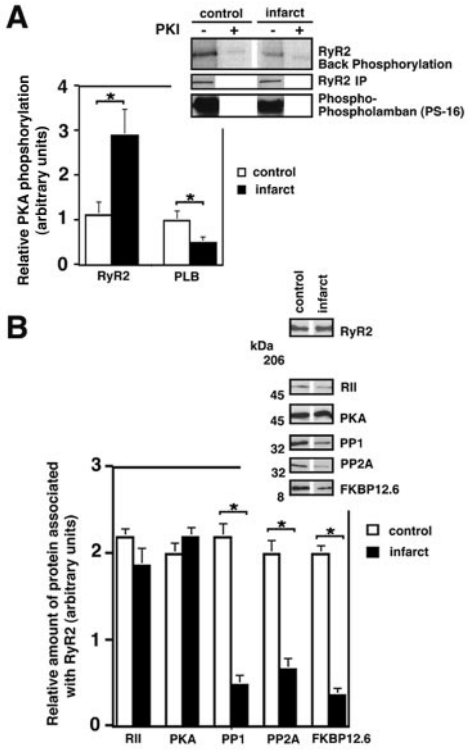

FIG. 3. **PKA phosphorylation of RyR2 and phospholamban in rat infarct (PMI) model of heart failure.** Myocardial infarction was created by ligation of the left anterior coronary artery in rats, which resulted in heart failure after 6 months (control rats were sham-operated). *A*, *upper panel* shows autoradiogram of back-phosphorylation of immunoprecipitated RyR2 with PKA and [γ-^{32}P]ATP with or without PKA inhibitor (*PKI*). The *middle panel* shows an immunoblot of immunoprecipitated RyR2 to confirm that equivalent amounts of RyR2 protein were present in each back-phosphorylation assay. The *lower panel* shows an immunoblot of heart lysate with anti-phospholamban antibody, which detects the phosphorylation of serine 16 (*PS-16*). The *bar graph* shows the relative PKA phosphorylation of RyR2 and phospholamban in the control and PMI groups. *B*, *upper right panels* are immunoblots of immunoprecipitations using anti-RyR antibody (5029) showing levels of components of the RyR2 macromolecular complex, including RyR2, the PKA regulatory subunit RII, PKA catalytic subunit, PP1, PP2A, and FKBP12.6. The accompanying *bar graph* shows the relative amounts of each of the components of the RyR2 macromolecular complex in failing and control hearts. *, $p < 0.01$ for the indicated comparison.

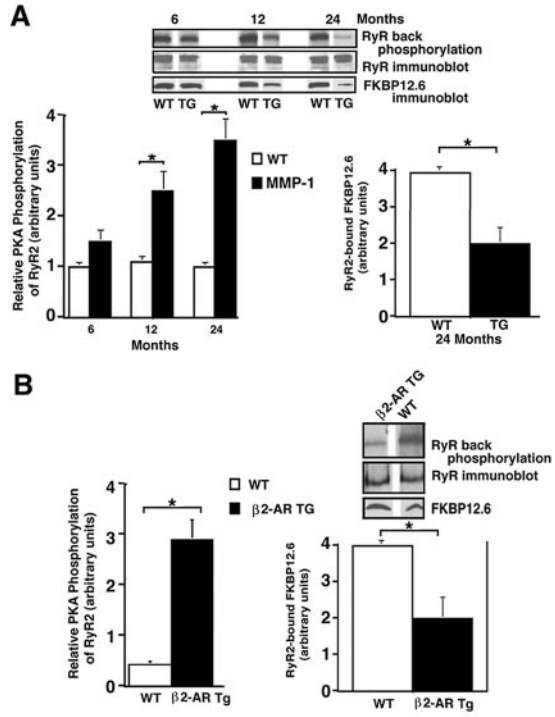

FIG. 4. **PKA phosphorylation of RyR2 in cardiac MMP-1 mouse model and β2-TG mice.** Mice with expression of human matrix metalloproteinase 1 (*MMP-1*) targeted to the heart develop progressive cardiac dysfunction over time (32). We examined RyR2 PKA phosphorylation and the content of FKBP12.6 in the RyR2 macromolecular complex over a 2-year time period. *A*, *upper panel* shows an autoradiogram of RyR2 that was immunoprecipitated from the MMP-1 transgenic (*TG*) and age-matched wild type litter mates and back-phosphorylated with PKA and [γ-^{32}P]ATP. The *middle panel* shows an immunoblot of immunoprecipitated RyR2 to confirm that equivalent amounts of RyR2 protein were present in each back-phosphorylation assay. The *lower panel* shows an immunoblot of FKBP12.6 in the RyR2-immunoprecipitated macromolecular complex. The *bar graph* at *left* shows the relative PKA phosphorylation of RyR2 at 6, 12, and 24 months of age. The *bar graph* at *right* shows relative levels of FKBP12.6 in the RyR2 macromolecular complex at 24 months of age. *B*, mice with overexpression of the β2-adrenergic receptor targeted to the heart (*β2-AR TG*) develop progressive cardiac dysfunction (50). The *upper right panel* shows an autoradiogram of RyR2 that was immunoprecipitated from transgenic (*β2-AR TG*) and age-matched wild type (*WT*) littermates and back-phosphorylated with PKA and [γ-^{32}P]ATP. The *lower two panels* are immunoblots of immunoprecipitations using anti-RyR antibody (5029) showing levels of RyR2 and FKBP12.6 in the RyR2 macromolecular complex. The *bar graph* at *left* shows the relative PKA phosphorylation of RyR2 in wild type and β2-AR TG mice. The *bar graph* at *right* shows relative levels of FKBP12.6 in the RyR2 macromolecular complex in wild type and β2-AR TG mice. *, $p < 0.01$ for the indicated comparison.

closely approximates acute βAR activation as shown in Fig. 1.

Our studies of human and canine heart failure (16) revealed changes in the cardiac RyR2 macromolecular complex, including PKA hyperphosphorylation of RyR2 and dissociation of FKBP12.6 from RyR2. Here we examined hearts from a rat model in which heart failure develops 6-month post-myocardial infarction (PMI) produced by ligation of the left anterior descending coronary artery. At 6 months PMI hearts were excised (following deep anesthesia) and immediately flash-frozen in liquid nitrogen. Fig. 3*A* shows PKA *hyper*phosphorylation of RyR2 and PKA *hypo*phosphorylation of PLB from the same hearts (Fig. 3*A*) providing additional evidence that RyR2 and PLB are differentially regulated with respect to PKA-dependent phosphorylation. The proteins of the macromolecular cluster involving RyR2 were also changed as shown in Fig. 3*B* (16). We found that FKBP12.6 was depleted from the RyR2 macromolecular complex in the failing rat hearts and there was a reduction in the levels of PP1 and PP2A (Fig. 3*B*), consistent with our previous reports concerning heart failure (16) but distinctive from cardiac hypertrophy (Fig. 2).

Mice with cardiac-specific expression of the human matrix metalloproteinase type 1 (MMP-1) develop progressive cardiac dysfunction over time (32). We measured PKA phosphorylation of RyR2 in these mice at 6, 12, and 24 months of age. Compared with age-matched WT littermates the MMP-1 TG mice exhibited progressively increasing PKA hyperphosphorylation of RyR2 (Fig. 4*A*) that correlated with the degree of cardiac dysfunction (32). Interestingly, even at 6 months, before hemodynamic compromise of the left ventricular function is detected, there was a trend toward increased PKA phosphorylation of RyR2 suggesting that this is an early event in the progression to heart failure. The PKA hyperphosphorylation of RyR2 was associated with a depletion of FKBP12.6 in the RyR2 macromolecular complex (Fig. 4*A*).

Mice with cardiac specific overexpression of the β2-adrenergic receptor (β2-AR TG) exhibit cardiac dysfunction that progresses with age and correlates with the degree of cardiac overexpression of the transgene (33). The overexpression of β2-AR leads to increased activity of PKA, because a fraction of

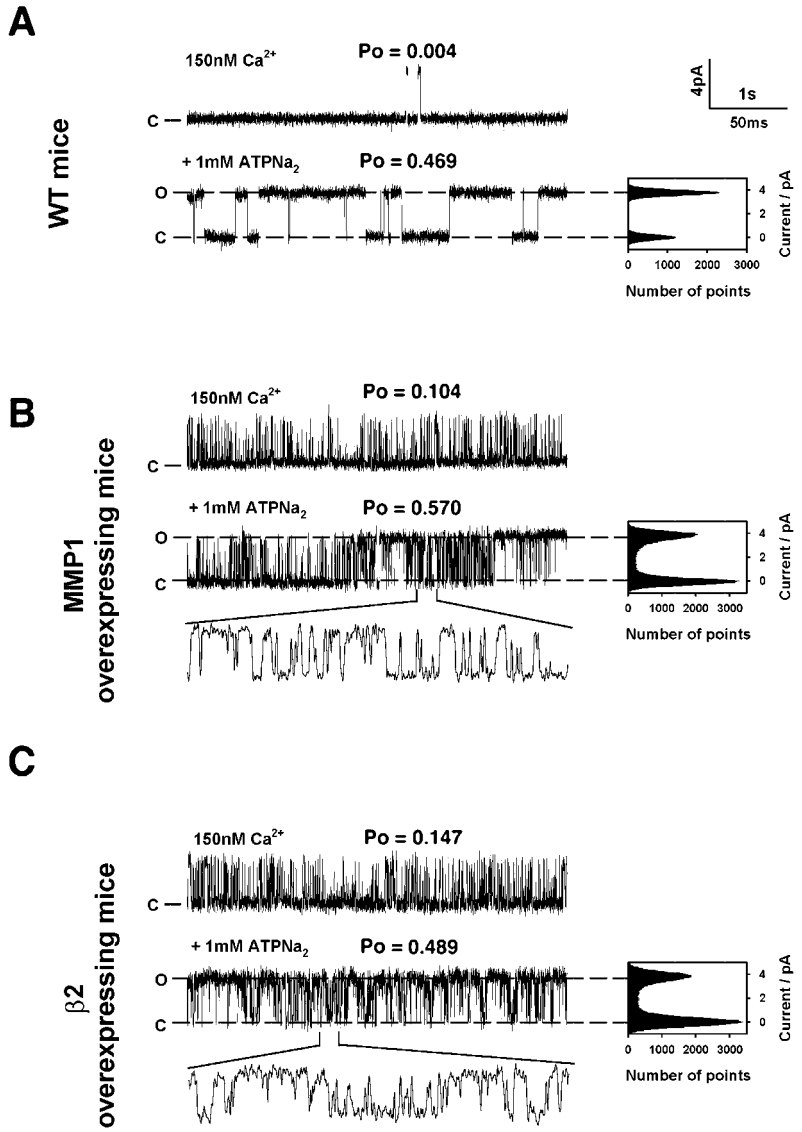

FIG. 5. **Single-channel properties of RyR2 from murine models that exhibit PKA-hyperphosphorylated RyR2.** *A*, RyR2 single channels from wild type mice examined in planar lipid bilayers show low activity at 150 nM $[Ca^{2+}]_{cis}$ corresponding to resting $[Ca^{2+}]$ during diastole in the heart in the *top tracing*. In the *bottom tracing* channels were activated with ATP, 1 mM, in the absence of Mg^{2+}. The amplitude histogram shown at the *right* of the *traces* indicates that channels exhibited two states fully closed (0 pA) and fully open (4 pA). *B*, RyR2 single channels from mice with cardiac-specific expression of MMP-1 exhibited increased activity (increased open probability, P_o) at 150 nM $[Ca^{2+}]_{cis}$, and the amplitude histogram shows evidence of partial openings or subconductance states seen when the channel is depleted of FKBP12.6 (6, 8, 16). *C*, RyR2 single channels from mice with cardiac-specific expression of β2-AR exhibited increased activity (increased open probability, P_o) at 150 nM $[Ca^{2+}]_{cis}$, and the amplitude histogram shows evidence of partial openings or subconductance states seen when the channel is depleted of FKBP12.6 (6, 8, 16). Values shown *above tracings* are for representative individual channels shown in this figure; mean values for all channels in each group are presented under "Results." Channels were recorded at 0 mV with Ca^{2+} as the current carrier, channel openings are upwards, and "*C*" denotes the closed state of the channel.

all β-ARs is activated even in the absence of agonist (33). That such activation occurs in this animal model is supported by the significant PKA hyperphosphorylation of RyR2 in the β2-AR TG mouse hearts (Fig. 4*B*). We found that RyR2 was PKA-hyperphosphorylated and that the RyR2 macromolecular complex was partially depleted of FKBP12.6 (Fig. 4*B*) consistent with the data presented above and those reported previously for human and canine RyR2 (16, 28). Taken together these data indicate that activation of the β2-AR signaling pathway in the mouse heart can result in PKA phosphorylation of RyR2 and depletion of FKBP12.6 from the RyR2 macromolecular complex.

To investigate the gating behavior of the PKA-hyperphosphorylated RyR2, we examined RyR2 single channel properties in planar lipid bilayers with low $[Mg^{2+}]$ (to increase P_o). Fig. 5 compared RyR2 gating from RyR2 from WT mouse hearts, MMP-1 transgenic mouse hearts and β2-AR transgenic mouse hearts. The RyR2 from WT are relatively PKA hypophosphorylated, and from MMP-1 and β2-AR transgenic mouse hearts RyR2 are PKA-hyperphosphorylated. FKBP12.6 was significantly depleted from the PKA-hyperphosphorylated RyR2 macromolecular complexes. Under control conditions with 150 nM *cis* (cytosolic) $[Ca^{2+}]$, the RyR2 channel activity was lowest in WT with an open probability (P_o) of 0.01 ± 0.01 (n = 12). RyR2 channel activity increased with PKA hyperphosphorylation of RyR2 and FKBP12.6 dissociation. The P_o was 0.35 ± 0.03 (n = 11) for MMP-1 RyR2, and 0.15 ± 0.04 (n = 14) for β2-AR RyR2 ($p < 0.001$ *versus* WT channels for both MMP-1 and β2-AR channels by ANOVA). ATP, in the absence of Mg^{2+} activates the RyR2 and we used the activation by 1 mM ATP in the continued presence of 150 nM $[Ca^{2+}]$ to further probe the behavior of the PKA phosphorylated RyR2. The P_o of WT was 0.47 ± 0.10 (n = 12), of MMP-1 was 0.55 ± 0.14 (n = 11) and β2-AR was 0.85 ± 0.14 (n = 14, $p < 0.001$ *versus* WT channels for both MMP-1 and β2-AR RyR2 channels by ANOVA). Thus PKA hyperphosphorylation of RyR2 is associated with increased RyR2 P_o regardless how the PKA-dependent phosphorylation was produced. These findings are consistent with the increase in P_o by PKA phosphorylation shown in RyR2 (19).

MMP-1 and β2-AR channels exhibit significantly faster gating kinetics (shorter open and closed events) compared with WT channels. The dwell time distributions for WT, MMP-1, and β2-AR channels exhibited three distinct dwell times ($\tau_1 < \tau_2 < \tau_3$) corresponding to three different open states and three different closed states of channels. All three mean open times (τ_o) were significantly longer for WT channels compared with MMP-1 and β2-AR channels (Table I). In addition, τ_{o2} and τ_{o3} for WT channels were one order of magnitude longer than the corresponding τ_{o2} and τ_{o3} exhibited by MMP-1 and β2-AR chan-

TABLE I
Ryanodine receptor open times

	τ_1[a]	τ_2	τ_3
		ms	
WT	0.91 ± 0.04 (12)	10.64 ± 0.62 (26)	142.86 ± 10.20 (62)
MMP-1	0.63 ± 0.01 (51)[b]	2.33 ± 0.10 (36)[b]	12.50 ± 1.41 (13)[b]
β2-AR	0.60 ± 0.01 (64)[b]	2.11 ± 0.07 (29)[b]	17.6 ± 1.67 (7)[b]

[a] Numbers in parentheses show the percentage of the total openings that each open state (τ_1, τ_2, and τ_3) accounts for based on analyses of the area under the curve for each dwell time as described under "Materials and Methods."
[b] $p < 0.01$ compared with WT channels.

TABLE II
Ryanodine receptor closed times

	τ_1[a]	τ_2	τ_3
		ms	
WT	0.51 ± 0.01 (17)	2.98 ± 0.09 (10)	169.50 ± 8.33 (73)
MMP-1	0.72 ± 0.01 (36)	4.65 ± 0.31 (36)[b]	16.39 ± 0.56 (28)[b]
β2-AR	0.98 ± 0.01 (32)	4.22 ± 0.12 (42)[b]	23.42 ± 1.08 (26)[b]

[a] Numbers in parentheses show the percentage of the total closings that each closed state (τ_1, τ_2, and τ_3) accounts for based on analyses of the area under the curve for each dwell time as described under "Materials and Methods."
[b] $p < 0.01$ compared with WT channels.

nels. MMP-1 and β2-AR channels never exhibited open states with mean open times longer than 100 ms; in contrast, 62% of the WT channel openings were to this long open state (Table I). MMP-1 and β2-AR channels preferentially occupied the open state with the shortest mean open time (Table I). Analyses of the closed states (τ_c) of the WT, MMP-1, and β2-AR channels revealed that τ_{c1} was significantly shorter for WT channels in comparison with MMP-1 and β2-AR channels (Table II), but τ_{c1} represented only 17% of the closings by WT channels. τ_{c2} and τ_{c3} were significantly longer for WT channels than the corresponding τ_c for MMP-1 and β2-AR channels. In addition, τ_{c3} for WT channels was one order of magnitude larger than for MMP-1 and β2-AR channels, exceeding 100 ms. MMP-1 and β2-AR channels never exhibited this long lasting closed state. MMP-1 and β2-AR channels exhibited equal distributions of each closed state, whereas 73% of the WT channel closings were to the longest closed state. Taken together these data are consistent with the destabilization of the MMP-1 and β2-AR channels due to PKA phosphorylation-induced dissociation of FKBP12.6 from the channels. In summary, PKA phosphorylation causes dissociation of FKBP12.6 from the RyR2 channel. FKBP12.6 stabilizes the RyR2 channel in both the closed and open state. Thus, when FKBP12.6 is removed from the channel due to PKA phosphorylation, both the open and closed times are shortened.

It is well established that isoproterenol response is markedly reduced in failing hearts (34), yet studies of heart failure tissues have reported effects of isoproterenol on cardiac contractility that are not observed *in vivo* (35). Possible explanations for this discrepancy are that RyR2 becomes dephosphorylated during the experiments and that the isoproterenol responses *ex vivo* or *in vitro* do not reflect the *in vivo* situation with respect to cardiac EC coupling. To test this hypothesis we examined the effects of isoproterenol on Ca^{2+} sparks in cardiomyocytes isolated from post-myocardial infarction (PMI) failing rat hearts in the absence of NaF. Based on our findings that RyR2 PKA hyperphosphorylation is lost during isolation of cardiomyocytes, we would predict that isoproterenol responsiveness would be restored in PMI cardiomyocytes isolated in the absence of NaF. Following isoproterenol application in PMI ventricular myocytes, Ca^{2+} sparks decayed more slowly (increased duration, $p < 0.001$), had smaller peak levels (decreased F/F_o, $p < 0.001$) and were wider (increased width, $p < 0.02$) (Fig. 6). These findings are consistent with reduced coupled gating between individual RyR2, which is a direct consequence of PKA phosphorylation-induced depletion of FKBP12.6 from the RyR2 macromolecular complexes (26, 27). In these studies isoproterenol was applied directly to the cardiomyocytes, so the problem of dephosphorylation of RyR2 during the isolation of cells was not an issue. The finding that isoproterenol has effects on Ca^{2+} sparks that are consistent with the effects of PKA phosphorylation of RyR2 as seen in bilayer experiments (16, 19) is in agreement with our finding that these RyR2 become dephosphorylated during the perfusion step required for cardiomyocyte isolation. If the RyR2 had remained PKA-hyperphosphorylated, the addition of isoproterenol would have had no additional affect on RyR2 channels as they would have been already essentially maximally PKA-phosphorylated. Although the biochemical assays are performed on flash-frozen hearts, the isolation of cardiomyocytes involves perfusion of the intact heart with a catecholamine-free solution and the cardiomyocytes are maintained in catecholamine-free culture media until use. During this time, the RyR2-bound phosphatases dephosphorylate the channel in the absence of NaF.

DISCUSSION

In this study we show for the first time that acute infusion of isoproterenol causes PKA phosphorylation of RyR2 and depletion of FKBP12.6 from the RyR2 macromolecular complex *in vivo*. PKA phosphorylation of RyR2 and depletion of FKBP12.6 from the RyR2 macromolecular complex are similar to the effects of RyR2 PKA hyperphosphorylation observed in human heart failure (16). The difference being that acute isoproterenol infusion is a transient effect, and the effects of heart failure generally persist for years. These data show that catecholamine release, as part of the "fight or flight" stress response, can modulate RyR2 function via PKA phosphorylation (Fig. 1).

Although acute administration of isoproterenol depletes the RyR2 macromolecular complex of FKBP12.6, it does not reduce the levels of phosphatases in the complex (Fig. 1), as occurs in the RyR2 complexes during chronic heart failure (16). Significantly, this finding points out a difference between the effects of acute administration of isoproterenol and heart failure, which is a chronic hyperadrenergic state. We found that, in contrast to experiments using flash-frozen heart samples, it was necessary to include the mild phosphatase inhibitor NaF, to preserve RyR2 PKA phosphorylation and FKBP12.6 dissociation following isoproterenol treatment using Langendorff perfusion of intact hearts. In contrast, PLB is also PKA-phosphorylated by the isoproterenol treatment, but its phosphorylation

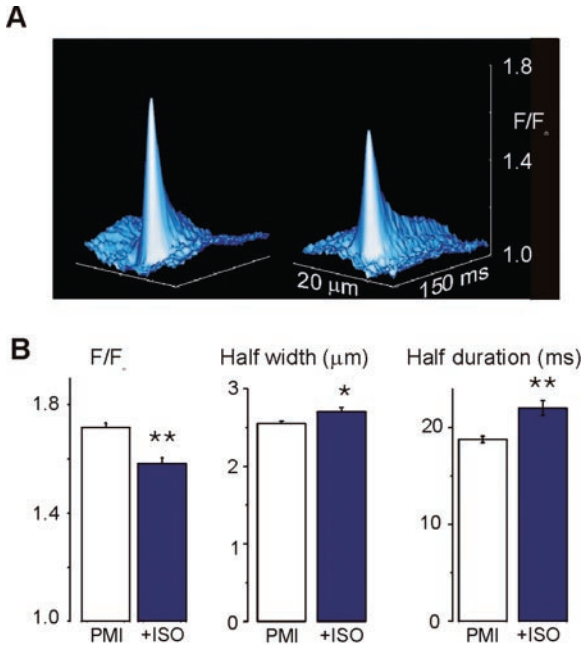

FIG. 6. **Ca^{2+} spark characteristics are modified in isolated PMI cardiomyocytes during β-adrenergic stimulation.** *A*, a three-dimensional projection of averaged Ca^{2+} sparks recorded in ventricular myocytes isolated from post-myocardial infarction (*PMI*) heart failure rats before (*left*, $n = 340$, recorded from eight cardiomyocytes) and after (*right*, $n = 164$, recorded from five cardiomyocytes) 1 μM isoproterenol application. *B*, *bar graph* showing from *left* to *right* the peak amplitude, half width, and half duration of Ca^{2+} sparks recorded in PMI myocytes before (*white bars*) and during (*blue bars*) isoproterenol application. *, $p < 0.05$; **, $p < 0.0001$.

state can be readily observed in the absence of a phosphatase inhibitor.

Thus, two important PKA phosphorylation targets, RyR2 and PLB, are regulated by distinct mechanisms. Because NaF was required to observe the increased PKA phosphorylation of RyR2 but not of PLB in cardiomyocytes isolated from control perfused hearts, our results suggest that the background phosphatase activity is relatively high for RyR2 but not for PLB. This distinction is likely explained by the fact that RyR2s comprise a macromolecular complex in which the phosphatases PP1 and PP2A are targeted directly to the channel (PKA, PP1, and PP2A bind to RyR2 via targeting proteins by virtue of leucine/isoleucine zippers (1)), and there is no evidence that phosphatases are targeted by a similar mechanism directly to PLB. Taken together these data support the concept that the RyR2-macromolecular complex is important in the regulation of local Ca^{2+} signaling in heart muscle. Moreover, these findings suggest that special care is needed when examining RyR2 PKA phosphorylation and the role of RyR2 PKA phosphorylation in cardiac signaling. For example, when cardiomyocytes are isolated from failing hearts using the widely accepted method of Langendorff perfusion, the RyR2 channels appear to become dephosphorylated.

It is important to stress that accurate measurement of PKA phosphorylation of RyR2 can be obtained without inhibition of phosphatases when cardiac tissue is immediately flash-frozen prior to measuring PKA phosphorylation of RyR2. This is the technique that we have routinely used to examine PKA phosphorylation of RyR2 in failing hearts (16, 28, 36, 37). Phosphatase inhibition is only required when measurements are made following isolation of cells or perfusion of intact hearts, when, in both circumstances, phosphatase activity in the RyR2 macromolecular complex can dephosphorylate the RyR2 channel and prevent accurate assessment of the *in vivo* level of PKA phosphorylation of RyR2. The finding that isoproterenol infusion *in vivo* results in PKA phosphorylation of RyR2 (Fig. 1, *C* and *D*), whereas perfusion of an intact heart *ex vivo* with isoproterenol results in only a small increase in PKA phosphorylation of RyR2 unless NaF is included in the perfusate, in which case there is equivalent PKA phosphorylation of RyR2 (Fig. 1, *A* and *C*), indicates that the balance of phosphorylation/dephosphorylation favors dephosphorylation under *ex vivo* conditions. Nevertheless, the significance of these findings are that, under *in vivo* conditions systemic isoproterenol can induce PKA phosphorylation of RyR2; under *ex vivo* conditions that are frequently used for experimental purposes it is important to inhibit the endogenous phosphatase activity to PKA phosphorylate RyR2.

We recognize that addition of NaF to the Langendorff perfusate could potentially alter signaling. To address this concern we ran the control experiment of perfusing with NaF alone and showed that there was no significant increase in PKA phosphorylation of RyR2. This indicates that, even if NaF activates adenylyl cyclase, as has been reported (38), there is no significant increase in PKA phosphorylation of RyR2 unless isoproterenol is added. Nevertheless, we cannot exclude the possibility that in some experiments part of the increase in PKA phosphorylation of RyR2 and PLB observed when NaF is added to the perfusate can be due to activation of adenylyl cyclase in addition to inhibition of phosphatases. However, as long as the appropriate controls are performed with each experiment, it should be possible to identify the contribution of NaF induced activation of PKA phosphorylation.

All models of heart failure that we have examined exhibit PKA hyperphosphorylation of RyR2 and dissociation of FKBP12.6 (16, 28, 36, 37). In end-stage human ischemic and idiopathic dilated cardiomyopathies, canine pacing-induced heart failure, and in the rat PMI model (shown here), there are also reductions of PP1 and PP2A in the RyR2 macromolecular complex. One implication of these findings is that the reduction of the phosphatases in the RyR2 macromolecular complex will tend to decrease the rate of dephosphorylation and contribute to the PKA hyperphosphorylation of RyR2 that is observed, even when the β-ARs may be down-regulated or desensitized.

The hypophosphorylation of PLB in PMI heart failure indicates that Ca^{2+} pumping into the SR will be decreased both by PLB-mediated inhibition of SERCA2a activity and by reduced levels of SERCA2a. The combination of PKA hyperphosphorylation of RyR2, which results in "leaky" SR Ca^{2+} release channels, decreased SERCA2a and PLB hypophosphorylation in heart failure can combine to contribute to decreased SR Ca^{2+} content (39) and decreased $[Ca^{2+}]_i$ transients (40).

When the RyR2 macromolecular complexes are depleted of FKBP12.6, the channels exhibit partial openings known as subconductance states. However, when RyR1 and FKBP12 were co-expressed in insect cells that lack endogenous FKBP12, these subconductance states were eliminated (6), and when FKBP12.6 was removed from RyR2 with FK506 or rapamycin subconductances appeared (8). Our results, indicating a cellular function for FKBP12/12.6 in the regulation of RyR1/RyR2 and establishing that functional Ca^{2+}-release channels are macromolecular complexes comprised of RyR and FKBP, have been confirmed by other laboratories (41–43). In addition to stabilizing RyR channels, FKBPs are required for coupled gating (26, 27). Coupled gating between RyR channels allows physically connected RyR channels to gate simultaneously (26, 27). Mathematical modeling of cardiac Ca^{2+} signaling (44) suggests that the presence of coupled gating is particularly important in terminating SR Ca^{2+} release from the large RyR2 clusters found in heart cells.

PKA phosphorylation of RyR2 increases the open probability of individual RyR2s in a cluster or Ca^{2+} release unit (CRU) such that for a given trigger Ca^{2+} the CRU is more likely to be activated and release SR Ca^{2+}. RyR2 channels are homotetramers comprised of four RyR2 subunits each of which binds one molecule of FKBP12.6 and contains a single PKA phosphorylation site (serine 2809) (16). When serine 2809 on RyR2 is PKA-phosphorylated, FKBP12.6 is dissociated from RyR2. The four equivalent PKA phosphorylation sites on each RyR2 channel provide the basis for a graded physiological response (21). In normal hearts, as each of the PKA sites is transiently phosphorylated there is a progressive physiological increase in RyR2 channel activity and increase EC coupling gain resulting in increased contractility. However, in failing hearts, where on average three or four of the PKA sites are chronically phosphorylated, and the channels are chronically depleted of FKBP12.6, they become destabilized or "leaky" (16). Under these conditions uncoupling of RyR2s would occur due to PKA hyperphosphorylation of RyR2 and depletion of FKBP12.6 from the macromolecular complex. As long as RyR2 is PKA-phosphorylated, FKBP12.6 cannot bind to the channel (1). This reduction in coupled gating (27) would decrease the probability of a CRU being activated by a trigger Ca^{2+} entering via the L-type channel and would increase the probability of diastolic openings of the SR Ca^{2+} release channels that could contribute (along with decreased SERCA2a activity) to depletion of SR Ca^{2+} content and provide signals that activate large inward depolarizing currents (EADs and DADs) that can trigger fatal cardiac arrhythmias associated with sudden cardiac death.

Our data are consistent with reduced coupled gating between individual RyR2 channels in failing hearts for the following reasons: 1) Coupled gating requires FKBP12.6 bound to RyR2, and we have shown that in failing hearts there is a reduction in the amount of FKBP12.6 bound to RyR2 due to PKA hyperphosphorylation. 2) The prolonged decay of calcium sparks in failing hearts can be explained by reduced coupled gating (see Ref. 44). Under normal conditions, the RyR2s in a cluster (CRU) will tend to be close together because of two factors: SR Ca^{2+} depletion and coupled gating. As coupled gating decreases, other factors being equal, RyR2s will be less well synchronized, and this will produce longer Ca^{2+} sparks and more variation in the Ca^{2+} spark duration. 3) Reduced coupling will tend to produce more RyR2 activation at low $[Ca^{2+}]_i$ and thus lead to some reduction of the amount of Ca^{2+} in the SR. This constitutes an increase in the "leak" of Ca^{2+} from the SR and a reduction in the average amount of Ca^{2+} in the SR. We suspect that it is the reduced SR Ca^{2+} content that leads to the reduction in peak Ca^{2+} spark fluorescence. In addition, the destabilization of individual channels resulting in decreased open and closed dwell times and subconductance states, due to the PKA phosphorylation-induced reduction in FKBP12.6 bound to the channels, may contribute to the alterations in spark characteristics as well.

A finding of considerable importance is the discovery that PKA phosphorylation of RyR2 correlates with the degree of cardiac dysfunction in a murine model. In the MMP-1 TG mouse model, which exhibits progressive cardiac dysfunction over time, RyR2 PKA phosphorylation gradually increases with the degree of cardiac dysfunction (Fig. 4*A*). This finding indicates that PKA phosphorylation of RyR2 may be an early finding in the progression to heart failure.

We found that channels from the MMP-1 and β2-AR transgenic mice that were PKA-hyperphosphorylated exhibited the same alterations in single-channel function (Fig. 5) as RyR2 channels isolated from failing canine and human hearts (16). These findings are consistent with the fact that both murine models exhibit cardiac dysfunction and support the concept that there is a causal relationship between chronic RyR2 PKA hyperphosphorylation and cardiac dysfunction in human HF and in animal models of HF. The major difference between the channels from control WT mouse heart and those from either the MMP-1 or β2AR transgenic mouse hearts is a decrease in open and closed dwell times. The gating of the channels from both the MMP-1 or β2-AR transgenic mouse hearts is dramatically different from that seen in the WT mouse heart controls due to this increase in gating frequency. Indeed, this is a characteristic finding for channels from failing hearts that are PKA-hyperphosphorylated and depleted of the stabilizing protein FKBP12.6 (16).

Our findings provide a new understanding of how stress-activated stimulation of the sympathetic nervous system regulates cardiac Ca^{2+} handling. Additionally, this work provides insight into the altered Ca^{2+} signaling that occurs in failing hearts. Although the present work addresses some of the mechanisms by which PKA-mediated signaling regulates RyR2 and Ca^{2+} homeostasis in heart, there are many additional changes produced by PKA activation besides the ones we have studied.

Our data are consistent with the reports of others regarding the effect of modulation of RyR2 function on EC coupling. A recent study from Bers and colleagues (45) reported that PKA phosphorylation of RyR2 has no effect on Ca^{2+} spark rate in murine cardiomyocytes at rest. However, these experiments were performed at extremely low cytosolic $[Ca^{2+}]$ levels (for reasons discussed below) of 10 and 50 nM. Thus, the most likely explanation for the failure to observe an effect of PKA phosphorylation on RyR2 is that PKA phosphorylation does not activate RyR2 when cytosolic $[Ca^{2+}]$ is maintained at artificially low levels (RyR2 is a Ca^{2+}-activated channel). This observation should not be extended to the more generalized statement that PKA phosphorylation does not activate RyR2 under physiological conditions that were not examined by Bers and colleagues. They used PLB null cardiomyocytes as well as cardiomyocytes expressing double mutant PLB that cannot be PKA-phosphorylated. They showed that cAMP-induced activation of PKA only modulated Ca^{2+} sparks when wild type (WT) PLB was present and, therefore, concluded that PKA phosphorylation of RyR2 has no functional effect. There are a number of possible explanations for the failure to observe an effect of PKA phosphorylation of RyR2 in this study, chief among them being the conditions of extremely low cytosolic $[Ca^{2+}]$ as noted above. Additional factors to consider in interpreting the results of Li *et al.* (45) include the fact that they used streptolysin-O to permeabilize cardiomyocytes. Streptolysin-O treatment resulted in cardiomyocytes with such high resting Ca^{2+} spark frequency that the studies had to be performed at 10 and 50 nM cytosolic $[Ca^{2+}]$, which is so low that normal RyR2 would be tightly shut. The presence of a high Ca^{2+} spark rate under their control conditions suggests that the SR was leaky and possibly damaged. Moreover, both the PLB null cells and the PLB double mutant are extreme cases in which there is either no PLB-mediated inhibition of SERCA2a or maximal PLB-mediated inhibition of SERCA2a. It is possible that under such extreme conditions the effects of PKA phosphorylation on RyR2-mediated SR Ca^{2+} release could be masked (*e.g.* by a drastic increase in SERCA2a activity that might reduce Ca^{2+} sparks or drastic decrease in SERCA2a activity that could impair SR Ca^{2+} uptake despite the fact that the authors attempted to control for these effects). An additional complexity arises due to the time dependence and $[Ca^{2+}]_i$ dependence of the effects of PKA phosphorylation of RyR2. Valdivia *et al.* (19) showed that, at low $[Ca^{2+}]_i$, the actions of PKA phosphoryla-

tion on RyR2 only were minimal. However, when $[Ca^{2+}]_i$ is rapidly increased (*e.g.* to 10 μM, see Ref. 44), there is a remarkable increase in RyR2 P_o, and this increase in P_o is much greater in PKA-phosphorylated RyR2. Furthermore, with maintained elevated $[Ca^{2+}]_i$ (which does not happen under physiological conditions) the effects of PKA phosphorylation are to reduce the P_o of RyR2. Thus, under the physiological conditions with only brief (~0.5–10 ms) elevations of "subspace" $[Ca^{2+}]$, the effects of PKA phosphorylation are to increase the P_o of RyR2.

The finding that acute administration of isoproterenol decreases Ca^{2+} spark heterogeneity (46) is also consistent with our data. The increased P_o of the RyR2 produced by PKA phosphorylation enhances the likelihood that a RyR2 cluster will be triggered by a local Ca^{2+} influx via dihydropyridine receptor (see above and Ref. 19). Additional rapid actions of PKA phosphorylation that also will produce this same "synchronization" action of isoproterenol are increased uptake of Ca^{2+} by the SR and increased SR Ca^{2+} content. Increase in luminal Ca^{2+} also increases RyR2 P_o (47, 48). Additional studies will be needed to determine how these multiple actions of PKA will effect synchronization, $[Ca^{2+}]_i$ transients, and Ca^{2+} sparks. Recent data from an FKBP12.6 null mouse (49) showing a significant increase in decay time of Ca^{2+} sparks in males are also consistent with our present findings.

Our earlier work showing that PKA activation may improve EC coupling in SS Dahl rat heart cells that exhibit signs of cellular heart failure (30) is also consistent with our present data. Indeed, the apparent paradox is resolved by our new findings. As noted in the results, the absence of NaF in the isolation medium in the previous study may have led to reversal of RyR2 PKA phosphorylation and of the FKBP12.6 dissociation. This would have the effect of restoring the isolated cells to the non-heart failure phenotype with respect to RyR2 function and explains why addition of PKA activators would have a beneficial effect.

The present study provides the first evidence of isoproterenol-induced RyR2 PKA phosphorylation *in vivo*, the importance of phosphatase inhibition in studies designed to measure RyR2-dependent Ca^{2+} signaling in cardiomyocytes isolated from failing hearts, and the correlation between progressive PKA phosphorylation of RyR2 and cardiac dysfunction. Moreover, we have presented our findings in the context of other recent studies. In so doing we propose a unifying concept of the role that defects in Ca^{2+} signaling, due to alterations in both Ca^{2+} release and reuptake, can play in the pathogenesis of heart failure and cardiac arrhythmias.

Acknowledgments—We thank P. Bideaux for performing the surgery in the rat infarct model and W. Koch and R. Lefkowitz for generously providing the β2-adrenergic receptor transgenic mice.

REFERENCES

1. Marx, S. O., Reiken, S., Hisamatsu, Y., Gaburjakova, M., Gaburjakova, J., Yang, Y. M., Rosemblit, N., and Marks, A. R. (2001) *J. Cell Biol.* **153,** 699–708
2. Marks, A. R., Tempst, P., Hwang, K. S., Taubman, M. B., Inui, M., Chadwick, C., Fleischer, S., and Nadal-Ginard, B. (1989) *Proc. Natl. Acad. Sci. U. S. A.* **86,** 8683–8687
3. Schreiber, S. (1991) *Science* **251,** 283–287
4. Jayaraman, T., Brillantes, A.-M. B., Timerman, A. P., Erdjument-Bromage, H., Fleischer, S., Tempst, P., and Marks, A. R. (1992) *J. Biol. Chem.* **267,** 9474–9477
5. Marks, A. R. (1996) *Physiol. Rev.* **76,** 631–649
6. Brillantes, A. B., Ondrias, K., Scott, A., Kobrinsky, E., Ondriasova, E., Moschella, M. C., Jayaraman, T., Landers, M., Ehrlich, B. E., and Marks, A. R. (1994) *Cell* **77,** 513–523
7. Timerman, A. P., Jayaraman, T., Wiederrecht, G., Onoue, H., Marks, A. R., and Fleischer, S. (1994) *Biochem. Biophys. Res. Commun.* **198,** 701–706
8. Kaftan, E., Marks, A. R., and Ehrlich, B. E. (1996) *Circ. Res.* **78,** 990–997
9. Gaburjakova, M., Gaburjakova, J., Reiken, S., Huang, F., Marx, S. O., Rosemblit, N., and Marks, A. R. (2001) *J. Biol. Chem.* **276,** 16931–16935
10. Hain, J., Onoue, H., Mayrleitner, M., Fleischer, S., and Schindler, H. (1995) *J. Biol. Chem.* **270,** 2074–2081
11. Hohenegger, M., and Suko, J. (1993) *Biochem. J.* **296,** 303–308
12. Islam, M. S., Leibiger, I., Leibiger, B., Rossi, D., Sorrentino, V., Ekstrom, T. J., Westerblad, H., Andrade, F. H., and Berggren, P. O. (1998) *Proc. Natl. Acad. Sci. U. S. A.* **95,** 6145–6150
13. Lokuta, A. J., Rogers, T. B., Lederer, W. J., and Valdivia, H. H. (1995) *J. Physiol.* **487,** 609–622
14. Marks, A. R. (2000) *Circ. Res.* **87,** 8–11
15. Marks, A. R. (2001) *J. Mol. Cell Cardiol.* **33,** 615–624
16. Marx, S. O., Reiken, S., Hisamatsu, Y., Jayaraman, T., Burkhoff, D., Rosemblit, N., and Marks, A. R. (2000) *Cell* **101,** 365–376
17. Takasago, T., Imagawa, T., and Shigekawa, M. (1989) *J. Biochem.* (*Tokyo*) **106,** 872–877
18. Takasago, T., Imagawa, T., Furukawa, K., Ogurusu, T., and Shigekawa, M. (1991) *J. Biochem.* (*Tokyo*) **109,** 163–170
19. Valdivia, H. H., Kaplan, J. H., Ellis-Davies, G. C., and Lederer, W. J. (1995) *Science* **267,** 1997–2000
20. Yoshida, A., Takahashi, M., Imagawa, T., Shigekawa, M., Takisawa, H., and Nakamura, T. (1992) *J. Biochem.* (*Tokyo*) **111,** 186–190
21. Marks, A. R., Reiken, S., and Marx, S. O. (2002) *Circulation* **105,** 272–275
22. Lederer, W. J., and Tsien, R. W. (1976) *J. Physiol.* (*Lond.*) **263,** 73–100
23. Wit, A. L., and Rosen, M. R. (1983) *Am. Heart J.* **106,** 798–811
24. Fozzard, H. A. (1992) *Basic Res. Cardiol.* **87,** 105–113
25. Pogwizd, S. M., Schlotthauer, K., Li, L., Yuan, W., and Bers, D. M. (2001) *Circ. Res.* **88,** 1159–1167
26. Marx, S. O., Ondrias, K., and Marks, A. R. (1998) *Science* **281,** 818–821
27. Marx, S. O., Gaburjakova, J., Gaburjakova, M., Henrikson, C., Ondrias, K., and Marks, A. R. (2001) *Circ. Res.* **88,** 1151–1158
28. Reiken, S., Gaburjakova, M., Gaburjakova, J., He, K. L., Prieto, A., Becker, E., Yi, G. H., Wang, J., Burkhoff, D., and Marks, A. R. (2001) *Circulation* **104,** 2843–2848
29. Alvarez, J. L., Aimond, F., Lorente, P., and Vassort, G. (2000) *J. Mol. Cell. Cardiol.* **32,** 1169–1179
30. Gomez, A. M., Valdivia, H. H., Cheng, H., Lederer, M. R., Santana, L. F., Cannell, M. B., McCune, S. A., Altschuld, R. A., and Lederer, W. J. (1997) *Science* **276,** 800–806
31. Schoenmakers, T. J., Visser, G. J., Flik, G., and Theuvenet, A. P. (1992) *BioTechniques* **12,** 870–4:876–9
32. Kim, H. E., Dalal, S. S., Young, E., Legato, M. J., Weisfeldt, M. L., and D'Armiento, J. (2000) *J. Clin. Invest.* **106,** 857–866
33. Rockman, H. A., Koch, W. J., and Lefkowitz, R. J. (1997) *Am. J. Physiol.* **272,** H1553–H1559
34. Newman, W. H., and Webb, J. G. (1980) *Cardiovasc. Res.* **14,** 530–536
35. Hasenfuss, G., Mulieri, L. A., Allen, P. D., Just, H., and Alpert, N. R. (1996) *Circulation* **94,** 3155–3160
36. Antos, C. L., Frey, N., Marx, S. O., Reiken, S., Gaburjakova, M., Richardson, J. A., Marks, A. R., and Olson, E. N. (2001) *Circ. Res.* **89,** 997–1004
37. Semsarian, C., Ahmad, I., Giewat, M., Georgakopoulos, D., Schmitt, J. P., McConnell, B. K., Reiken, S., Mende, U., Marks, A. R., Kass, D. A., Seidman, C. E., and Seidman, J. G. (2002) *J. Clin. Invest.* **109,** 1013–1020
38. Brostrom, C. O., Brostrom, M. A., and Wolff, D. J. (1977) *J. Biol. Chem.* **252,** 5677–5685
39. Hobai, I. A., and O'Rourke, B. (2001) *Circulation* **103,** 1577–1584
40. Yao, A., Su, Z., Nonaka, A., Zubair, I., Spitzer, K. W., Bridge, J. H., Muelheims, G., Ross, J., Jr., and Barry, W. H. (1998) *Am. J. Physiol.* **275,** H1441–H1448
41. Ahern, G. P., Junankar, P. R., and Dulhunty, A. F. (1997) *Biophys. J.* **72,** 146–162
42. Shou, W., Aghdasi, B., Armstrong, D. L., Guo, Q., Bao, S., Charng, M. J., Mathews, L. M., Schneider, M. D., Hamilton, S. L., and Matzuk, M. M. (1998) *Nature* **391,** 489–492
43. Chen, L., Molinski, T. F., and Pessah, I. N. (1999) *J. Biol. Chem.* **274,** 32603–32612
44. Sobie, E. A., Dilly, K. W., Dos Santos Cruz, J., Lederer, W. J., and Jafri, M. S. (2002) *Biophys. J.* **83,** 59–78
45. Li, Y., Kranias, E. G., Mignery, G. A., and Bers, D. M. (2002) *Circ. Res.* **90,** 309–316
46. Litwin, S. E., Zhang, D., and Bridge, J. H. (2000) *Circ. Res.* **87,** 1040–1047
47. Xu, L., and Meissner, G. (1998) *Biophys. J.* **75,** 2302–2312
48. Gyorke, I., and Gyorke, S. (1998) *Biophys. J.* **75,** 2801–2810
49. Xin, H. B., Senbonmatsu, T., Cheng, D. S., Wang, Y. X., Copello, J. A., Ji, G. J., Collier, M. L., Deng, K. Y., Jeyakumar, L. H., Magnuson, M. A., Inagami, T., Kotlikoff, M. I., and Fleischer, S. (2002) *Nature* **416,** 334–338
50. Koch, W. J., Lefkowitz, R. J., Milano, C. A., Akhter, S. A., and Rockman, H. A. (1998) *Adv. Pharmacol.* **42,** 502–506